GEOLOGICAL
SOCIETY OF NORWAY

Configuration of the Scandinavian Ice Sheet in southwestern Norway during the Younger Dryas

Jason P. Briner[1], John Inge Svendsen[2], Jan Mangerud[2], Henriette Linge[2], Richard Gyllencreutz[3], Svein Olaf Dahl[4] & Derek Fabel[5]

[1] Department of Geology, University at Buffalo, Buffalo, NY USA

[2] Department of Earth Sciences, University of Bergen and Bjerknes Centre for Climate Research, Bergen, Norway

[3] Department of Geological Sciences and The Bolin Centre for Climate Research, Stockholm University, Stockholm, Sweden

[4] Department of Geography, University of Bergen and Bjerknes Centre for Climate Research, Bergen, Norway

[5] Scottish Universities Environmental Research Center, University of Glasgow, Scotland

E-mail corresponding author (Jason Briner) jbriner@buffalo.edu

The extent of the Scandinavian Ice Sheet in southwestern Norway is precisely located during the well-characterized Younger Dryas re-advance. However, the thickness of the ice sheet is less well constrained inland from the terminal position. Some exceptions include lateral moraines traced inland and up to 1000 m a.s.l. along Hardangerfjorden. Here, we apply ^{10}Be dating in two areas: (1) bedrock and boulders in the high-relief landscapes near the Younger Dryas margin around the Bergen urban area, and (2) boulders from an upland 1600 m a.s.l. much farther (120 km) inland. We find that coastal summits ranging from ~400 to ~680 m a.s.l. and located only ~10–15 km up-flow from the ice margin, were covered by the Scandinavian Ice Sheet during the Younger Dryas. The scatter in the ^{10}Be age population of 22 boulder samples is best explained by isotopic inheritance owing to inefficient subglacial erosion during the prior glaciation. Most of the 11 bedrock samples also exhibit inheritance, pointing to the source of inheritance in boulders and implying inefficient subglacial erosion during the last glaciation even in valley-bottoms near Bergen. Regional glacial striae compilations suggest that ice flow during maximum Younger Dryas ice-sheet configurations was for the most part cross-valley, with potentially low basal slip rates. Five new ^{10}Be ages from the inland site help to constrain ice height far inland. We combine these new results with prior information to generate a cross profile of the Younger Dryas ice sheet in southern Norway.

Introduction

Ice sheets are part of important climate feedback mechanisms that lead to sharp latitudinal contrasts in temperature. Despite their significant role in the Earth's climate system, our understanding of their configuration – particularly their height – through time and space is still limited (Hughes et al., 2016, Dalton et al., 2020, Clark et al., 2022). Geological observations of past ice-sheet configuration remain critical for validating and improving climate modeling (e.g., Sommers et al., 2021), for elucidating glacio-isostatic adjustment of the crust that is critical for understanding the causes of relative sea-level change (Gowan et al., 2021; Fjeldskaar & Amantov, 2018), for constraining post-glacial immigration of flora and fauna (Alsos et al., 2022), and for predicting spatial patterns of future sea-level changes (e.g., Caron et al., 2018).

The history of Scandinavian Ice Sheet margin fluctuations during the last deglaciation is reasonably well known in coastal southwestern Norway (Fig. 1). The Bergen area was deglaciated at around 14 ka (Mangerud et al., 2017), and remained ice-free for 2000 years with an ice-sheet position at least 40 km east of Bergen (Mangerud et al., 2019). Subsequently, during the Younger Dryas, the ice sheet re-advanced and built the Herdla Moraine close to the outer coast ~11.6 ka (Mangerud et al., 2016; Fig. 2). The Bergen area became ice free again ~11.5 ka as the ice front retreated rapidly inland in response to Holocene warming (Mangerud et al, 2019).
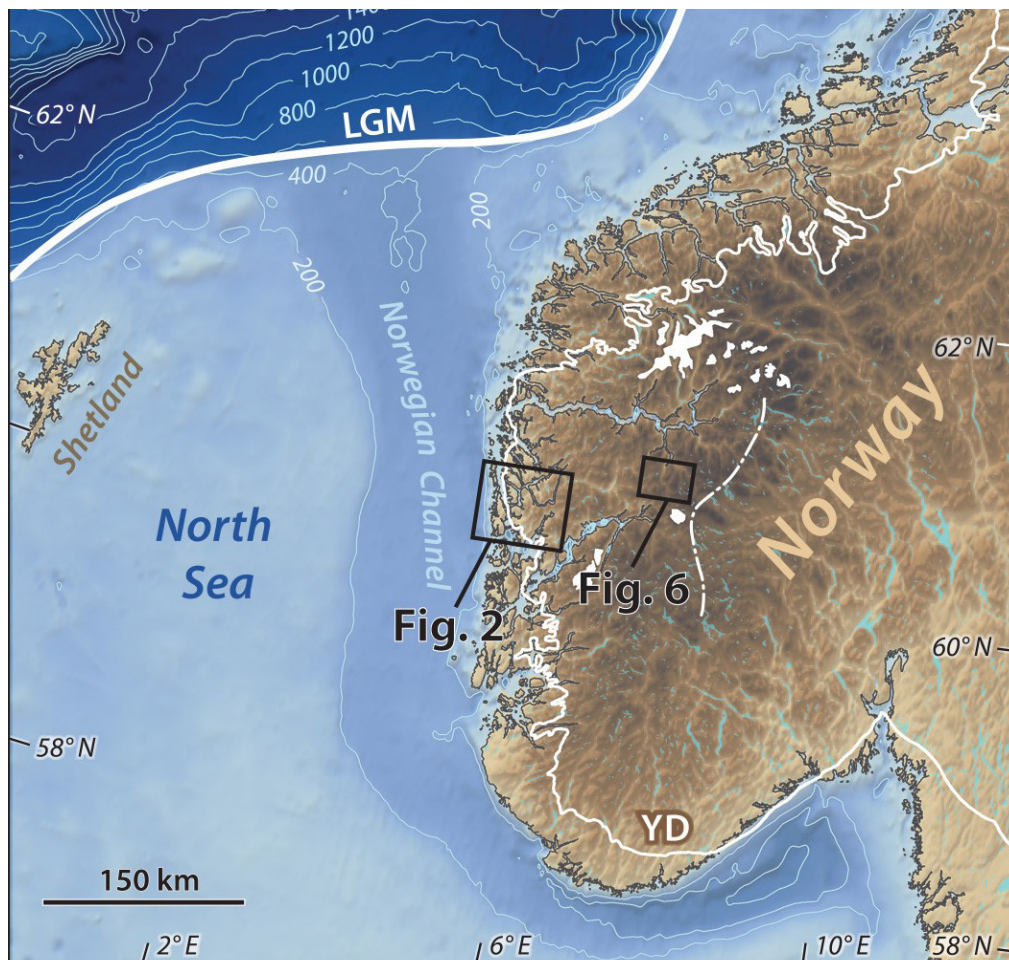

Figure 1. Map of southern Norway and the North Sea showing the extent of the Scandinavian Ice Sheet during the Last Glacial Maximum (LGM) and Younger Dryas (YD). The dashed white line shows the assumed Younger Dryas ice divide.
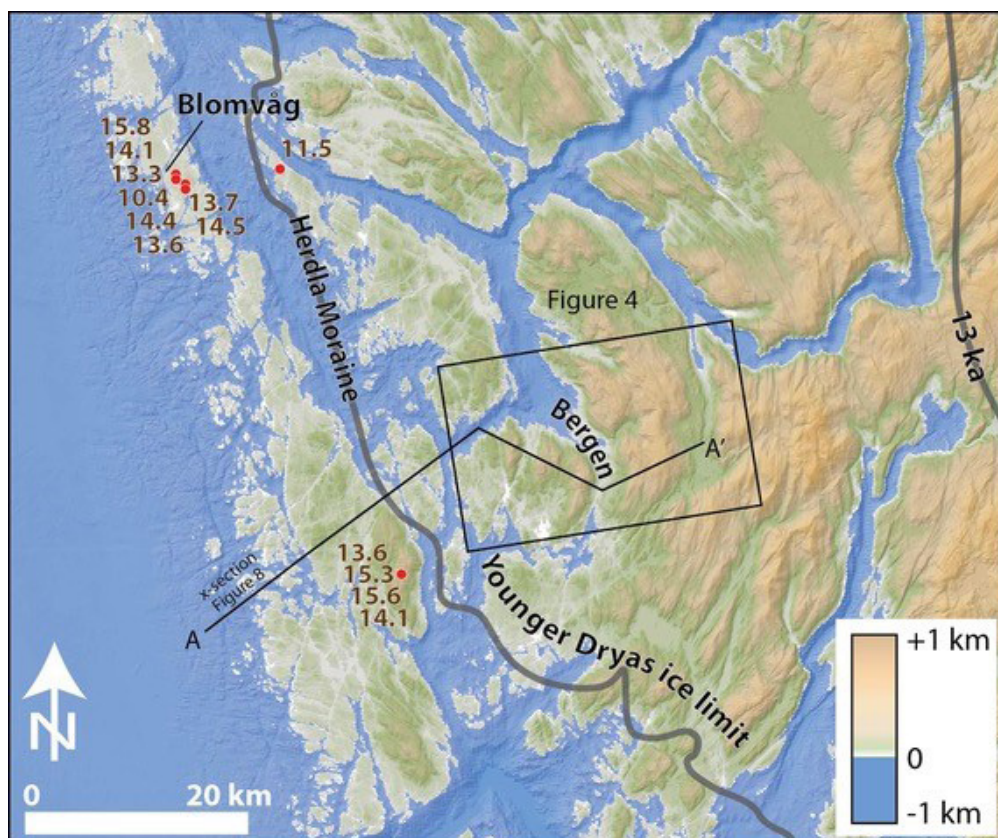
Figure 2. Map showing the extent of the Younger Dryas ice limit in the Bergen area of southwestern Norway (from Mangerud et al., 2016), along with previously published 10Be ages (re-calculated here) from Mangerud et al. (2017). 13 ka limit from Mangerud et al. (2019). The topography of the A–A' line is shown in Fig. 8.

The timing and lateral extent of the Younger Dryas re-advance is better documented in the Bergen-Hardanger area than any other place around the Scandinavian Ice Sheet. Lateral moraines also show the slope of the ice surface along Hardangerfjorden (Follestad, 1972; Mangerud et al., 2013). However, the steepness of the ice margin, and the height of the ice sheet during this event, remains largely under-constrained in the topographically complex area around Bergen, i.e., between the two large fjords Hardangerfjorden and Sognefjorden. What was the Younger Dryas ice-sheet profile in the Bergen area and how might this guide knowledge of the shape of the Scandinavian Ice Sheet during the Younger Dryas?

The main aim of this study has been to resolve this question by [10]Be-exposure-dating of erratic boulders found on the highest mountains close to the Younger Dryas ice margin, i.e., mountains around the city of Bergen. We also include [10]Be-ages from erratics on higher mountain peaks farther inland to determine the height of the ice surface. In other projects, [10]Be ages had been obtained from lower elevations in the area overrun by the Younger Dryas re-advance. We include these results, as well as new radiocarbon ages from a key stratigraphic section, because they improve our understanding of inheritance of [10]Be in our samples and they also represent a first step in quantifying glacial erosion in such a landscape.

Background

The Scandinavian Ice Sheet covered most, if not all, coastal mountains in western Norway during the Last Glacial Maximum (Hughes et al., 2016; Regnéll et al., 2021). Ice flowed across the Bergen area from the higher elevations to its east and advanced onto the continental shelf in the North Sea. Once offshore, this inland ice was confluent with the north-flowing Norwegian Channel Ice Stream, which terminated at the continental shelf break on the southern flank of the Norwegian Sea ~250 km down flowline from Bergen (Fig. 1) (Sejrup et al., 2003). In this section, we synthesize previously published age constraints to generate two alternative exposure histories for the highest mountains in the Bergen area (Fig. 3) from which to compare our suite of new [10]Be ages. We outline this history in three stages:

Stage 1 – pre–Younger Dryas deglaciation

Sejrup & Hjelstuen (2022) depict the recession of Norwegian Channel Ice Stream west of Bergen between 19 and 18 ka. Despite this relatively early post-LGM recession, available data indicate that the ice margin did not recede inside the outermost islands in this area until between ~15 and ~14 ka (Mangerud et al., 2017). At the village of Blomvåg in Øygarden (Fig. 2), basal marine sediments have radiocarbon ages of 14.1 ± 0.2 cal ka BP [re-calibrated using Marine20 (Brendryen et al., 2020)] supported by [10]Be ages from nearby erratic boulders that average 14.0 ± 1.4 ka (Mangerud et al., 2016). Following deglaciation of the western coastline, the ice front continued to retreat at least ~40 km inland (east) of the Bergen area. Near Bergen, the oldest radiocarbon ages from re-worked shells found in or below a till associated with the Younger Dryas re-advance cluster at ~14.0 cal ka BP (Mangerud et al., 2016).

Stage 2 – Younger Dryas re-advance

The youngest among about 90 radiocarbon ages on shells re-worked into a till deposited during the Younger Dryas re-advance the Bergen-Hardangerfjorden area date to ~12.5 cal ka BP (Mangerud et al., 2016). This indicates that the ice sheet advanced across the Bergen area shortly after 12.5 cal ka BP. Relative sea-level curves showing a 10 m rise that culminated at the end of Younger Dryas
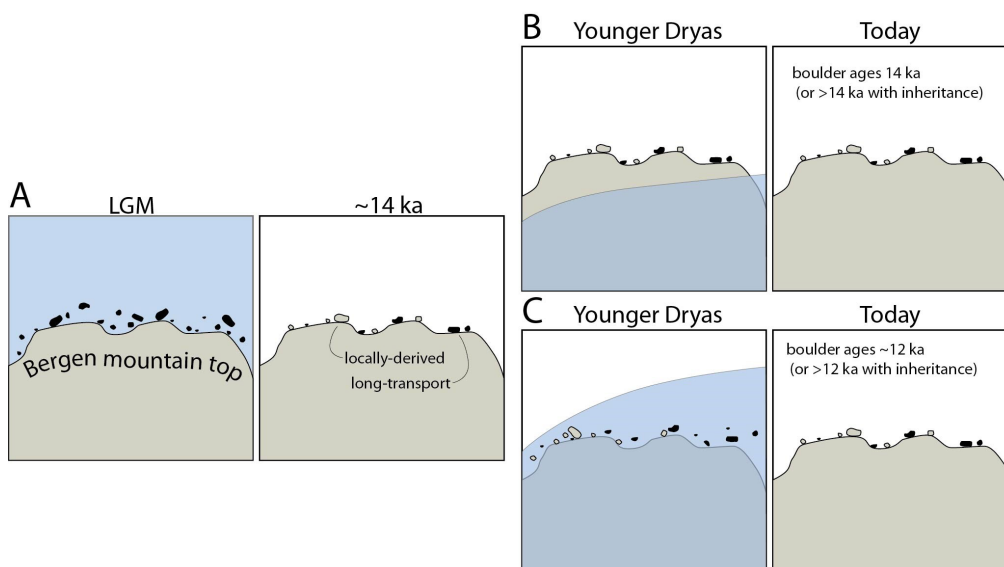

Figure 3. Ice-sheet cover scenarios for mountain summits in the Bergen area, depicting locally derived glacially transported boulders (gray, higher possibility of having [10]Be inheritance) and long-transported glacial boulders (black, lower possibility of having [10]Be inheritance). (A) Ice free at 14 ka. (B) Ice free during the Younger Dryas. (C) Ice covered during the Younger Dryas.

suggest that the re-expansion of the Ice Sheet started during the Allerød interstadial period (Lohne et al., 2007). The ice margin continued to expand westward to a position ~12 km down flowline from Bergen (Fig. 2). There are multiple lines of evidence indicating that the re-advance attained its maximum extent shortly before the transition to the Holocene; in some areas, Younger Dryas maximum phase sediments were deposited stratigraphically well above the Vedde Ash (12.1 cal ka) (Bondevik & Mangerud, 2002; Lohne et al., 2004), and in other areas, ice-marginal deposits rest on *in situ* shells dating to ~12 cal ka (Mangerud et al. 2016).

How thick the Younger Dryas ice was around the city of Bergen is unknown and allows for two different exposure histories. If adjacent summits were not re-occupied during the Younger Dryas, then exposure ages of perched boulders should be ~14 ka (and with inheritance, potentially older; Fig. 3). If, on the other hand, summits were re-occupied during the Younger Dryas, then boulders without inheritance should have exposure ages of ~11.5 ka (Fig. 3).

Stage 3 – Recession from the Younger Dryas

The timing of ice recession has been dated precisely from plotting the elevation of raised ice-marginal deltas in a well-dated "master" shore-line diagram (Mangerud et al., 2019), indicating that the Bergen area was deglaciated between 11.5 and 11.4 cal ka BP.

Methods

^{10}Be dating

We sampled bedrock surfaces and perched boulders on or near the highest summits in the Bergen area, which lies slightly within the Younger Dryas ice extent (Fig. 4). High topographic areas below former ice sheets are challenging landscapes for cosmogenic-nuclide exposure dating, because cosmogenic-nuclide accumulation can survive multiple glacial cycles due to minimal glacial erosion (e.g., Brook et al., 1996; England, 1999; Briner et al., 2005; Fabel et al., 2006; Goehring et al., 2008).
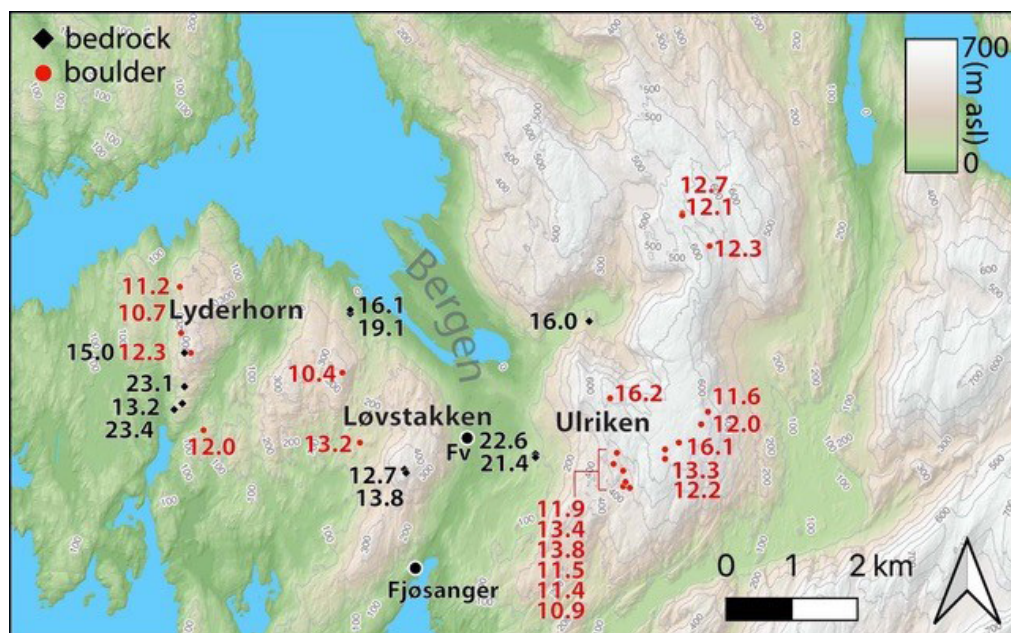

Figure 4. Map of Bergen region showing ^{10}Be ages of bedrock (black diamonds) and perched boulders (red circles). Fv = Fjøsangerveien site.

Thus, our sampling strategy includes sampling many perched erratic boulders. Our bedrock samples are from various elevations, allowing assessment of the relative magnitude of glacial erosion efficiency, and hence inheritance and its potential influence on boulder age distributions. Our dataset consists of 22 [10]Be ages from boulders from 49 to 677 m a.s.l., and 11 [10]Be ages from bedrock surfaces from 90 to 477 m a.s.l. (Fig. 5). At all sites, sampled boulders rested directly on bedrock that exhibited evidence of erosive subglacial conditions. To constrain the inland height of the ice sheet, we supplemented the Bergen dataset with five samples from erratic boulders from the mountain Tarven in a tributary valley to Sognefjorden, which is a high mountain near the center of the ice sheet that serves the purpose of constraining ice-sheet thickness. Tarven is a logistically feasible location with suitable boulders that are located 1234–1620 m a.s.l. ~120 km up flowline and serve as a test of inland ice-sheet height during the Younger Dryas (Fig. 6).

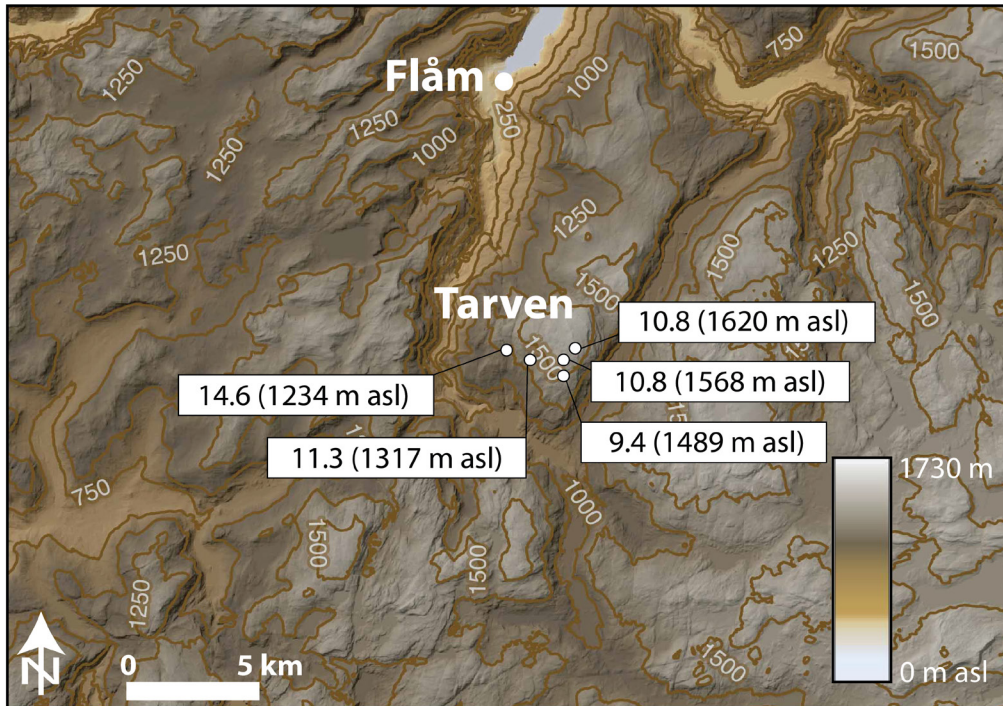Figure 5. Selected photos of field locations and samples.

Figure 6. Map showing location of Tarven and ^{10}Be ages (in ka). Map location shown in Figure 1.

We collected samples with an angle grinder, hammer and chisel. Subsequent sample processing took place in two labs, one in Buffalo, USA and one in Glasgow, UK. Both labs follow similar quartz purification and beryllium isolation protocols (Kohl & Nishiizumi, 1992; Corbett et al., 2016). Samples processed in Buffalo had beryllium ratios measured at the Center for Accelerator Mass Spectrometry in Livermore, California, US. BER samples were processed and measured at the Scottish Universities Environmental Research Centre, East Kilbride, UK. Table 1 includes metadata about AMS standards and other sample-specific information.

We calculate all ^{10}Be ages using the ^{10}Be production rate of Goehring et al. (2011, 2012) and version 3 of the online exposure age calculator (https://hess.ess.washington.edu/; Balco et al. 2008). This applies both to ages we report here for the first time and those previously published. We use the "Goehring rate" and the Lal/Stone scaling scheme (referred to hereafter as Lm; Lal, 1991; Stone, 2000) to be consistent with calculations used at other sites in western Norway. The "Goehring rate" is an average rate calibrated locally in western Norway at two sites, one of which is a Younger Dryas moraine with independent radiocarbon age control, and one is a rock fall deposit at 6.0 cal ka BP that killed a tree that was radiocarbon dated (Nesje, 2002). Other production rate choices include the "Scandinavian rate" of Stroeven et al. (2015) or the "Arctic rate" of Young et al. (2013) or the "global rate" from the CRONUS project (this is the default rate in the age calculator v3), among others. We favor the Goehring rate due to the proximity of the calibration sites, but note that it is higher than other rates, and thus yields the youngest ages among the production rate choices [e.g., ~6 % younger than the "global" rate of Borchers et al. (2016) and 2–3 % younger than the "Scandinavian" rate of Stroeven et al. (2015)].

Table 1. Beryllium-10 exposure age sample information

Site Name	Surface type	Sample ID	Latitude	Longitude	Sample dimension (HxLxW, m)	Sample lithology	Elevation (m)	Thickness (cm)	Shielding	Year of collection	10Be (atoms/gram of quartz)	10Be uncertainty (atoms/gram of quartz)	AMS standard	10Be age
Lyderhorn	bedrock	BER_0901	60,364027	5,241086	NA	Tonalitic gneiss	187	2,0	0,9997	2009	138310,1	5308,9	NIST_30600	23430 ± 905
Lyderhorn	bedrock	BER_0902	60,373546	5,242021	NA	Tonalitic gneiss	400	3,0	1,0000	2009	108566,6	4083,3	NIST_30600	15021 ± 567
Lyderhorn	bedrock	BER_0903	60,367845	5,242606	NA	Tonalitic gneiss	196	4,0	0,9978	2009	135302,8	5964,7	NIST_30600	23123 ± 1025
Lyderhorn	bedrock	BER_0904	60,364896	5,242891	NA	Tonalitic gneiss	163	2,0	0,9991	2009	76404,8	4790,5	NIST_30600	13237 ± 833
Isdalen	bedrock	BER_0907	60,389080	5,375840	NA	Quartzite	135	1,0	0,9833	2009	88892,7	4431,4	NIST_30600	15986 ± 800
Løvstakken	bedrock	BER_1001	60,359010	5,321720	NA	Augen gneiss	477	4,0	1,0000	2010	106215,0	4338,0	NIST_30600	13785 ± 565
Løvstakken	bedrock	BER_1002	60,359389	5,321350	NA	Augen gneiss	469	2,5	0,9996	2010	98507,4	3410,4	NIST_30600	12728 ± 442
Laksevåg	bedrock	BER_1003	60,384334	5,295000	NA	Augen gneiss	92	3,0	0,9915	2010	100593,8	4681,8	NIST_30600	19090 ± 893
Laksevåg	bedrock	BER_1004	60,384093	5,295082	NA	Augen gneiss	90	1,0	0,9915	2010	86072,7	4118,5	NIST_30600	16092 ± 773
Langhaugen	bedrock	BER_1105	60,365160	5,364270	NA	Quartzite	107	8,0	0,9954	2011	116604,0	3672,6	NIST_30600	22613 ± 716
Langhaugen	bedrock	BER_1107	60,365200	5,363890	NA	Quartzite	105	1,5	0,9950	2011	116228,8	3394,6	NIST_30600	21439 ± 630
Damsgårdsfjellet	boulder	BER_1005	60,374162	5,295430	1.3x3.0x1.8	local gneiss	334	1,5	0,9999	2010	71572,0	2630,8	NIST_30600	10413 ± 384
Krohnegården	boulder	BER_0908	60,362851	5,304918	1.7x2.0x1.0	local gneiss	152	5,0	0,9953	2009	73553,3	4492,1	NIST_30600	13255 ± 812
Askøy	boulder	BER_0909	60,543811	4,988825	1.8x2.5x2.5	local gneiss	49	5,0	0,9970	2009	57644,9	3671,2	NIST_30600	11529 ± 736
Kanadaskogen	boulder	BER_0906	60,361035	5,251593	1.8x3.0x2.5	local gneiss	129	2,0	0,9995	2009	67154,3	3228,2	NIST_30600	12040 ± 580
Lyderhorn	boulder	80-L17	60,38437	5,23655	2.5x1.5x1.0	local gneiss	237	1,5	1,0000	2015	63704,7	1805,2	07KNSTD	11158 ± 317
Lyderhorn	boulder	81-L18	60,37367	5,24293	2.0x2.0x1.7	local gneiss	384	1,1	1,0000	2015	80897,1	1541,9	07KNSTD	12251 ± 234
Lyderhorn	boulder	81-L19	60,37693	5,23924	3.0x3.0x4.0	local gneiss	311	1,5	1,0000	2015	65465,5	1284,6	07KNSTD	10664 ± 210
Ulriken	boulder	U-15	60,404330	5,412630	2.5x1.5x1.0	local gneiss	636	2,0	1,0000	2015	101532,6	4006,6	07KNSTD	12283 ± 486

Ulriken	boulder	U-16	60,409080	5,402040	2.0x0.7x1.1	local gneiss	589	2,0	1,0000	2015	100713,0	4611,7	07KNSTD	12710±584
Ulriken	boulder	U-17	60,409080	5,402040	3.0x1.6x1.5	local gneiss	507	2,0	1,0000	2015	88861,3	3884,9	07KNSTD	12086±530
Ulriken	boulder	78-U1	60,36783	5,40849	4.0x2.0x2.0	local gneiss	638	2,4	1,0000	2015	100561,5	1677,9	07KNSTD	12185±204
Ulriken	boulder	78-U2	60,3693	5,40805	2.5x1.5x1.4	local gneiss	641	2,3	1,0000	2015	110056,3	2092,8	07KNSTD	13289±254
Ulriken	boulder	78-U3	60,37079	5,41252	2.0x1.3x1.5	local gneiss	653	2,2	1,0000	2015	134691,7	2544,9	07KNSTD	16079±305
Ulriken	boulder	78-U4	60,37649	5,42018	1.0x1.0x0.8	not local gneiss	677	2,4	1,0000	2015	99063,9	1889,1	07KNSTD	11593±222
Ulriken	boulder	78-U5	60,37444	5,41871	2.0x1.2x1.5	local gneiss	670	2,6	1,0000	2015	101446,9	1931,2	07KNSTD	11965±228
Ulriken	boulder	80-U6	60,3765	5,38684	1.2x0.8x0.6	local gneiss	634	2,4	1,0000	2015	132857,7	2625,5	07KNSTD	16158±321
Ulriken	boulder	94-U7	60,36567	5,39155	2.0x1.6x1.4	local gneiss	412	2,0	1,0000	2015	90225,8	2123,6	07KNSTD	13411±317
Ulriken	boulder	94-U9	60,36773	5,39171	1.2x0.8x1.0	not local gneiss	474	2,0	1,0000	2015	84609,5	2094,7	07KNSTD	11867±295
Ulriken	boulder	94-U11	60,36218	5,39565	5.0x4.0x2.0	local gneiss	404	2,0	1,0000	2015	75995,0	1788,5	07KNSTD	11380±269
Ulriken	boulder	U12	60,36267	5,39598	2.5x1.2x1.2	local gneiss	401	2,0	1,0000	2015	76814,4	1472,6	07KNSTD	11535±222
Ulriken	boulder	U13	60,36475	5,39434	2.5x2.0x1.2	local gneiss	545	2,0	1,0000	2015	105105,5	2003,9	07KNSTD	13810±264
Ulriken	boulder	U14	60,36225	5,39777	5.0x4.0x4.0	local gneiss	401	2,0	1,0000	2015	72853,4	1394,6	07KNSTD	10939±210
Tavern	boulder	T-2020-1	60,769765	7,184177	ND	local gneiss	1620	1,5	1,0000	2020	203364	5728	07KNSTD	10819±306
Tavern	boulder	T-2020-2	60,765424	7,177273	ND	local gneiss	1568	2,0	1,0000	2020	194864	6100	07KNSTD	10838±340
Tavern	boulder	JIS_T1	60,7596786	7,1782909	1.0x1.0x0.8	local gneiss	1489	2,0	1,0000	2020	158341	4048	07KNSTD	9375±241
Tavern	boulder	JIS_T3	60,76340	7,15456	2.3x2.0x1.0	quartzite	1317	1,5	1,0000	2020	166669	3985	07KNSTD	11265±270
Tavern	boulder	JIS_T4	60,76635	7,13657	2.5x2.0x1.5	local gneiss	1234	1,5	1,0000	2020	201801	4509	07KNSTD	14585±327

Sample density used is 2.65 grams/cc, surface erosion is zero, atmospheric model is "std." Ages calculated using production rate of Goehring et al (2012) and "Lm" scaling. See text for link to web calculator. The lithology of most boulder samples is gneiss; "not local" indicaters field evaluation that lithology does not appear to be locally derived. The bedrock lithologies can be obtained here: https://geo.ngu.no/kart/berggrunn_mobil/. None of the bedrock/ boulder surfaces sampled show striations, the degree of weathering/erosion is too advanced, i.e. quartz veins typically protrude 1–3 cm above the gneiss surface.

Radiocarbon dating

We exploited a temporary sediment section in the Bergen valley (informal site name Fjøsangerveien) at the entrance of a new tunnel for a light rail (60.358213° N, 5.340767° E) into the mountain Løvstakken. An excavation (Figs. 5 & 7) was created from the surface to bedrock exposing up to 8 m of sediments that we subdivide into three units (lower, middle, upper). The lower unit, which rests directly on bedrock, is a compact diamicton dominated by subangular pebbles and boulders. This is draped by a middle unit (22–25 m a.s.l.) that is a 2–3 m-thick clay-rich, ice-drop diamicton that can be followed laterally throughout the exposure. It is somewhat deformed and tectonized. In places, it contains high concentrations of in situ marine mollusc shells, mainly *Chlamys islandica*. Other species include *Mytilus edulis*, which requires influx of temperate Atlantic water and a seasonal ice-free zone to thrive (Mangerud & Svendsen, 2017). The shell-bearing sediments are covered by a meter-thick dark gray layer that mostly consists of silt and clay and is void of shells. The section is capped by the upper unit, which is a massive and compact diamicton up to 4 meters thick and densely packed with subangular gravel particles, stones, and boulders. Rooted in this diamicton are large granitic boulders that bear evidence of glacial transportation.
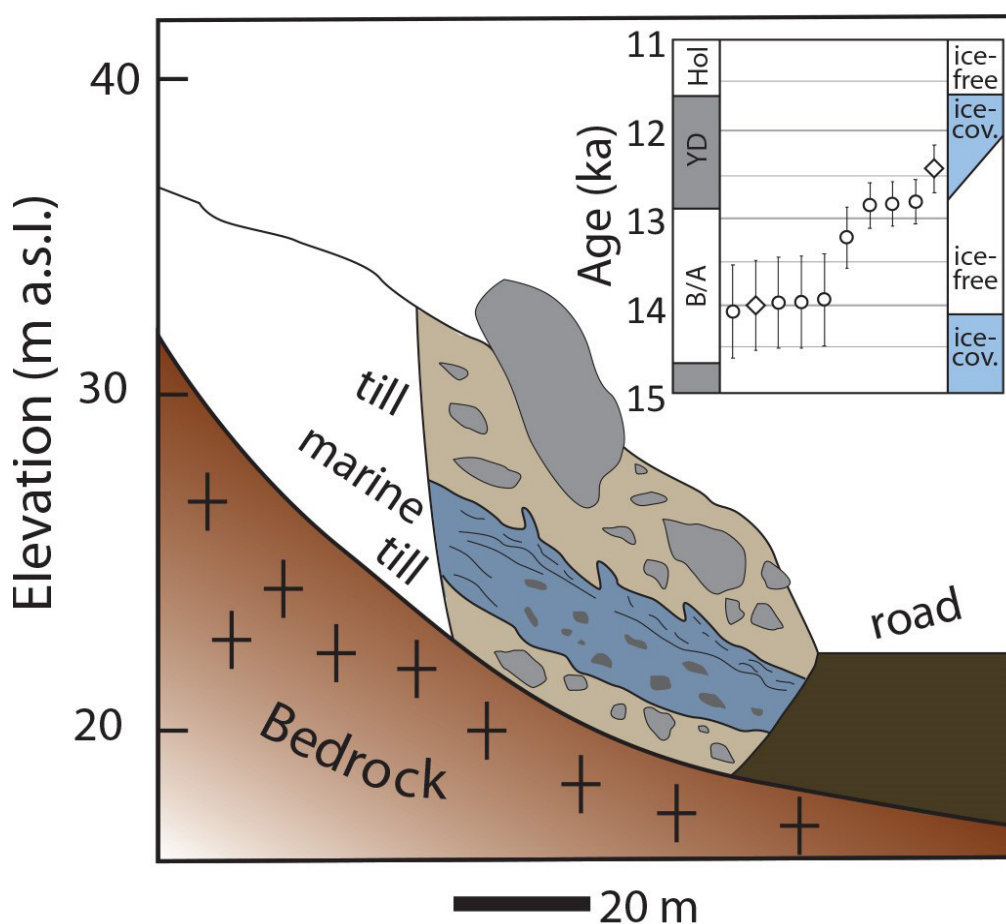

Figure 7. The sediment section temporarily exposed at Fjøsangerveien. Inset shows eight calibrated radiocarbon ages on marine material collected from this outcrop (circles) and two calibrated radiocarbon ages from marine shells re-worked into till exposed in a sediment section nearby (diamonds; Mangerud et al., 2016). Ages reported in Table 2; photo of Fjøsangerveien section in Fig. 5.

We obtained eight radiocarbon ages from the shell-bearing unit, including five mollusc shells and three samples from different parts of a growth layer of a calcareous algae (*Lithohamnion* sp) enclosing a pebble. The samples were from different parts of the exposed strata, but not in stratigraphic order. We calibrate radiocarbon ages <12,200 ^{14}C yr BP using Marine20 (Heaton et al., 2020), and ages >12,200 using the Normarine18 calibration (Brendryen et al., 2020). Additionally, for comparison, we re-calibrate two previously published radiocarbon ages that were collected very near the sampled new section described here (11,020 ± 60 and 12,750 ± 60 yr BP), reported in Mangerud et al. (2016). Radiocarbon ages were measured at the Radiocarbon Dating Laboratory, Lund University, Sweden.

Results

[10]Be ages

The 22 new [10]Be ages of boulders in the Bergen area range from 10.4 ± 0.4 to 16.2 ± 0.3 ka with an average age of 12.4 ± 1.4 ka (Table 1; Fig. 4). On the Ulriken summit, the highest mountain in the Bergen area, where the majority (15) of our boulder samples are from, the ages range from 10.9 ± 0.2 to 16.2 ± 0.3 ka and average 12.8 ± 1.6 ka. The elevations of the Ulriken samples range from 401 to 677 m a.s.l. Eliminating six boulders (five too old, one too young) following Chi-squared analysis (using version 3 of the online calculator; https://hess.ess.washington.edu/) results in a mean of 11.8 ± 0.9 ka of the remaining nine Ulriken boulders. There is no relationship between sample age and elevation ($r^2 = 0.17$).

The 11 bedrock samples have apparent [10]Be ages that range from 12.70.4 to 23.4 ± 0.9 ka, of which seven samples pre-date 15 ka. All surfaces exhibit evidence of glacial erosion from sliding ice. The elevations of the bedrock samples range from 90 to 477 m a.s.l. Samples with apparent ages older than 15 ka lie between 90 and 200 m a.s.l.

Five boulders from our inland site are from elevations spanning 1234 to 1620 m a.s.l., and [10]Be ages range between 9.4 ± 0.2 and 14.6 ± 0.3 ka (Fig. 6). Eliminating two boulders (one too old, one too young) following Chi-squared analysis reported on version 3 of the online calculator (https://hess.ess.washington.edu/) results in a mean of 11.0 ± 0.2 ka for the remaining three boulders.

Radiocarbon ages

The sediment section Fjøsangerveien is interpreted as containing a lower and upper till with a glaciomarine unit between (Fig. 7). Four shell dates from the glaciomarine unit yield ages of around 14,000 cal kyr BP whereas one yields a younger age of around 13,200 cal kyr BP (Table 2). The three radiocarbon ages from the clast coated with *lithohamnium* algae yield identical ages of around 12,800 yrs BP.

Table 2. Radiocarbon ages of marine fossils in the Bergen valley

Lab ID	Sample details	Conventional 14C age (yr)	Uncertainty (1 sigma)	2 sigma age range (yr)	Midpoint of largest 95.4 range (yr)	Half of largest 95% range (yr)	Source
Poz-24281	Minde, *Mya truncata* reworked in till	11020	60	12196-12732 (95.4)	12464	268	Mangerud et al. (2016)
Poz-24282	Minde, *C. islandica* reworked in till	12750	60	13503-14520 (95.4)	14012	509	Mangerud et al. (2016)
LuS-14908	Fjøsangerveien-1, *Chlamys islandica*	12700	70	13464-14493 (95.4)	13979	515	This study
LuS-14909	Fjøsangerveien-2, *Mya truncata*	12690	70	13456-14488 (95.4)	13972	516	This study
LuS-14910	Fjøsangerveien-3, *Mytilus edulis*	12850	70	13555-14600 (95.4)	14078	523	This study
LuS-18304	Fjøsangerveien-2022-1-*Lithothamnium*-outer	11610	60	12613-13110 (95.4)	12862	249	This study
LuS-18305	Fjøsangerveien-2022-2-*Lithothamnium*-inner	11640	80	12616-13135 (95.4)	12876	260	This study
LuS-18306	Fjøsangerveien-2022-4-*Lithothamnium*-outer	11560	80	12583-13091 (95.4)	12837	254	This study
LuS-18307	Fjøsangerveien-2022, *Hiatella arctica*	12650	70	13424-14469 (95.4)	13947	523	This study
LuS-18308	Fjøsangerveien-2022, *Mya truncata*	12050	80	12901-13587 (94.7), 13889-13845 (0.8)	13244	343	This study

Note: Calibration information: 0–12190 cal a BP: Marine20 -133 ± 54 (14C yr BP ± 1sigma), 12200–21240 cal a BP: Normarine18 (14C yr BP ± 1sigma); uncertainty propagated by taking root sum of squares.

Discussion

Beryllium-10 ages, inheritance and glacial erosion

Prior results demonstrate that valleys in the Bergen area were finally deglaciated at ~11.5 ka, following the ice sheet re-advance to the Herdla end moraine system during the Younger Dryas (Mangerud et al., 2019). Thus, [10]Be ages from bedrock surfaces in the lower elevations near Bergen should date to ~11.5 ka if they have experienced sufficient glacial erosion, on the order of 2–3 m (Briner et al., 2016), during the preceding glacial overriding. Alternatively, if surfaces were minimally eroded during the Younger Dryas advance, they should date to ~14.5 ka, their first deglaciation following the longer overriding during the Last Glacial Maximum. In fact, most [10]Be ages from bedrock surfaces, all of them glacially sculpted, pre-date not only 11.5 ka, but also 14.5 ka, by thousands of years (Fig. 4). This stands in clear contradiction to our new radiocarbon ages from the Fjøsangerveien site, which lies close to our nearby bedrock site with ages of ~22 ka (Fig. 4). We interpret these anomalously high bedrock ages as being influenced by varying amounts of isotopic inheritance, and thus consider them as apparent ages only. We find it plausible that the glacier erosion was less than 2–3 m during this last ice-sheet advance that probably covered Bergen for only a few hundred years during the late Younger Dryas.

Many of the apparent [10]Be ages pre-date ~14 ka, implying inefficient erosion also during the Last Glacial Maximum, which is unexpected. Five samples in valley bottom locations range between ~16 and ~23 ka, indicating relatively inefficient subglacial erosion during the Last Glacial Maximum even in the valley bottom. This valley bottom inheritance may relate to the protected nature of these valleys as regional ice flow for long periods was mostly across, not along, the investigated valleys (Wirsig et al., 2017). This is supported by the preserved last interglacial sediments at Fjøsanger (Mangerud et al., 1981; Fig. 4), proving that at least parts of these valley bottoms were not eroded during the last glaciation. The remaining bedrock samples, from surfaces on summit ridges west of Bergen, have apparent [10]Be ages that are equally old (~23 ka) and others that range between ~13 and ~15 ka.

Were the summits near Bergen ice-covered during the Younger Dryas?

The mean (~11.8 ± 0.9 ka) of the 9 accepted [10]Be ages from boulders perched on the bedrock surfaces on Ulriken's mountain plateau is statistically inconsistent with an age of ~14 ka for the deglaciation of the summit. Our new radiocarbon ages confirm previous dating results indicating that the Bergen valley became ice free in the late Bølling, a little before 14,000 yrs ago and remained ice free until sometime after 12,500 yrs BP when the ice sheet advanced towards the Herdla Moraine (Mangerud et al., 2016). Taken together, these results show that the highest summits adjacent to Bergen were ice covered for some period during the Younger Dryas. We selected large boulders resting in stable positions perched directly on bedrock surfaces, and there is little to no sediment cover on the uplands surrounding Bergen. Shielding by snow would require snowpack thicknesses and snow densities that are inconsistent with meteorological data and with observations of large boulders being windswept even during in the snowiest months of the year. We therefore find no plausible explanation for boulder ages that are ~2000 years younger than the deglaciation age if the mountain peaks remained ice free during the Younger Dryas. The seven additional boulders from adjacent summits in the Bergen area similarly post-date ~14 ka. We thus interpret the distribution of [10]Be ages as supporting the view that all summits around Bergen were ice covered during the Younger Dryas. We note that most boulders that failed the Chi-squared test pre-date the mean age, which is expected given the levels of inheritance found in bedrock samples.
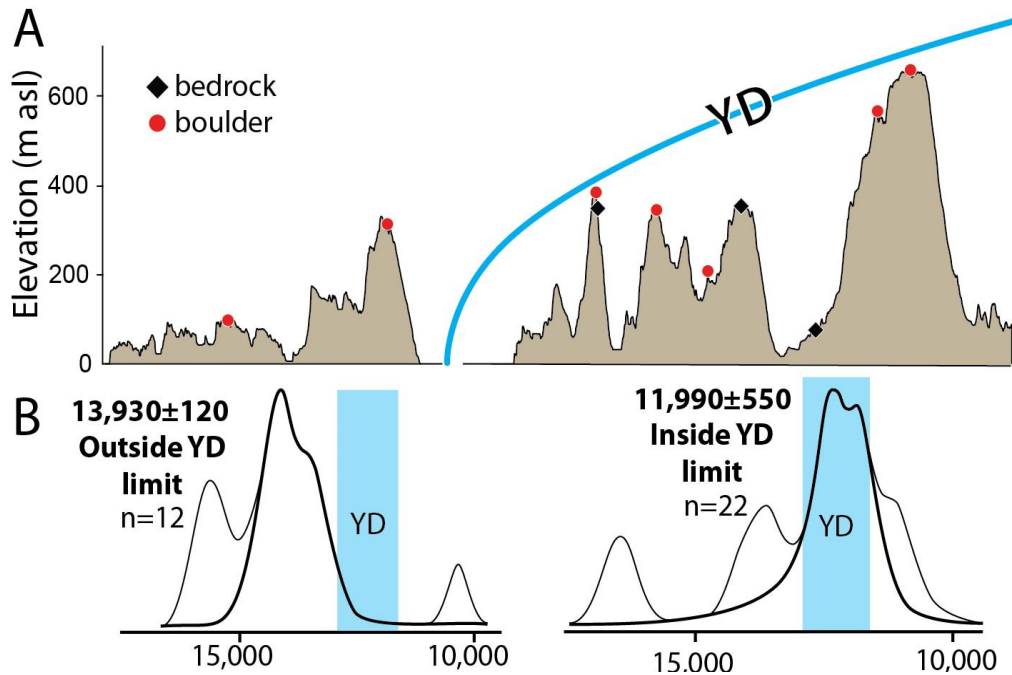
Figure 8. (A) Topographic cross-section across the Younger Dryas ice limit and a simplified depiction of the Younger Dryas ice-sheet profile (profile location shown in Fig. 2); sample localities within and beyond the Younger Dryas ice limit are shown. (B) [10]Be age distributions within (right) and beyond (left) the Younger Dryas ice extent; thin lines are statistical outliers (see text).

Bolstering our interpretation of summits being occupied by ice during the Younger Dryas is the comparison of boulder age distributions beyond vs. within the mapped Younger Dryas margin. Twelve [10]Be ages from boulders west of the Younger Dryas ice margin average 14.0 ± 1.4 ka (Mangerud et al., 2017). Using the same Chi-squared criteria as above to exclude four outliers (three too old, one too young), the remaining eight boulder samples have a mean age of 13.9 ± 0.1 ka (Fig. 8). This mean age is statistically distinct from the mean age 12.0 ± 0.6 ka of the boulders within the Younger Dryas margin, all from summit positions (Fig. 8). We note that the boulders west of the Younger Dryas margin are statistically overlapping with the independent ^{14}C age control on the deglaciation of that area of 14.1 ± 0.2 cal ka BP, indicating that the [10]Be chronometer (and production rate that we employ) is working well in that landscape.

Ice sheet or local ice?

These dating results alone cannot distinguish whether the summits were covered by the Scandinavian Ice Sheet or simply by local glaciers. The Younger Dryas equilibrium-line altitude has been estimated in middle Hardangerfjorden to be at ~1300 m a.s.l. (Mangerud et al., 2013; Regnéll et al., 2021). This elevation is well above the Ulriken plateau (~600 m a.s.l.). However, the Younger Dryas snowline lowered considerably seaward. At the island Stord, ~50 km south of Bergen and along a similar uplift isobase (Mangerud et al., 2016), the Younger Dryas equilibrium-line altitude is estimated to be only ~500 m a.s.l., which is below the elevation of the Ulriken plateau (~600 m a.s.l.). Thus, based on an assessment of the glaciation limit during the Younger Dryas it is not unreasonable to assume that the Ulriken plateau hosted a local ice cap that merged with the adjacent ice sheet, as was the case for the ~1200 m a.s.l. Ulvanosa massif in outer Hardangerfjorden (Regnéll et al., 2021) and in other coastal uplands in coastal western Norway (Mangerud, 2023). A compilation of hundreds of glacial striae in the Bergen area

(Mangerud et al., 2019), on the other hand, shows a pattern of mostly uniform ice flow from inland to coast, and does not display a radial pattern expected to be produced by a local ice source on Ulriken or other summits. Nor are there any obvious local moraines that could indicate local ice cap glaciation. We are nevertheless open to the possibility that a local ice cap formed on top of Ulriken at some time, but the consistent west-oriented striae shows that the entire mountain plateau was overrun by the Scandinavian ice Sheet during its most recent episode of ice cover.

Ice-sheet geometry during the Younger Dryas

We next discuss the ice-sheet profile geometry of the Younger Dryas ice margin and farther inland. Previous studies that reconstruct ice-sheet height in this area have focused mainly on Hardanger-fjorden (Mangerud et al., 2013; Aakesson et al., 2018, 2020; Regnéll et al., 2021). Here, ice-surface slopes are comparable to the contemporary ice-sheet outlet glacier Sermeq Kajulleq (Jakobshavn Isbræ), Greenland. We reconstructed a surface slope of the Younger Dryas ice-marginal area near Bergen, consistent with our dating results, to rise above the studied summits (Fig. 9). This profile is only slightly steeper than the ice-sheet profile along Hardangerfjorden based on mapping of lateral moraines. This implies that despite ice being channeled through that ~5 km-wide fjord system, the ice sheet still had a basal shear stress comparable to what it had while flowing across the more rugged terrain near Bergen. We also note that our ice-sheet profile is steeper and higher than that of Fjeldskaar & Amantov (2018), which also depicts ice that is too thin at the Tarven site.

We leverage the two-dimensional ice-margin profile reconstruction with previously published information to reconstruct a surface contour map of the westernmost part of the Scandinavian Ice Sheet during the Younger Dryas (Fig. 9). The map is a slight modification and an extension of the maps by Hamborg & Mangerud (1981) and Fareth (1972) and it is based on the following types of observations: The pattern of the Younger Dryas end moraines, the positions and slopes of lateral moraines and the directions of glacial striae considered to represent Younger Dryas ice flow, with glaciologically plausible interpretations, are in line with the general glacial geology of the area. Much of the map's contours are interpolated between sites with height information, and we see the reconstruction as the best available field-based map that can be compared with ice-sheet model simulations. Along Hardangerfjorden, lateral moraines are mapped from sea level and up to 1000 m a.s.l. (Follestad, 1972; Regnéll et al., 2021), constraining an ice-profile that is similar to the surface profile of Jakobshavn Isbræ (Mangerud et al. 2013). Along Samnangerfjorden (Fig. 9), lateral moraines are traced up to 600 m a.s.l. and along Fanafjorden (Fig. 9) lateral moraines are traced up to 300 m a.s.l. (Hamborg & Mangerud, 1981; Mangerud et al., 2019; Aarseth & Mangerud, 1974). We interpolated and extrapolated these profiles and altitudes along the ice margin. Between Samnangerfjorden and Fensfjorden (Fig. 9), the Younger Dryas end moraines show a wide and quite regular lobe form, which is reflected in the directions of the glacial striae, including striae on Ulriken and other mountains, pointing at right angles to the moraines (Mangerud et al., 2019; Aarseth and Mangerud, 1974).

Well inland, our new [10]Be ages from high elevations post-date the Younger Dryas. Previously published [10]Be ages from boulders on adjacent mountain uplands are 11.2 ka (1354 m a.s.l.; 60.9042°, 7.2764°) and 10.5 ka (1569 m a.s.l.; 60.9851°, 7.2817°) (Andersen et al. 2018); these ages have been re-calculated to be consistent with the calculation method used here. Collectively, these data also confirm a Younger Dryas ice height above these elevations. More broadly, we know of no robust evidence that would demand the height of the ice sheet during the Younger Dryas to be lower than southern Norway's topography. Rather, if one uses the modern-day Greenland Ice Sheet as a guide, we suggest that the height of the ice-sheet surface during the Younger Dryas could likely have been well above southern Norway's topography. To investigate this further, we selected a transect in southern Greenland that has many commonalities with southern Norway during the Younger Dryas:
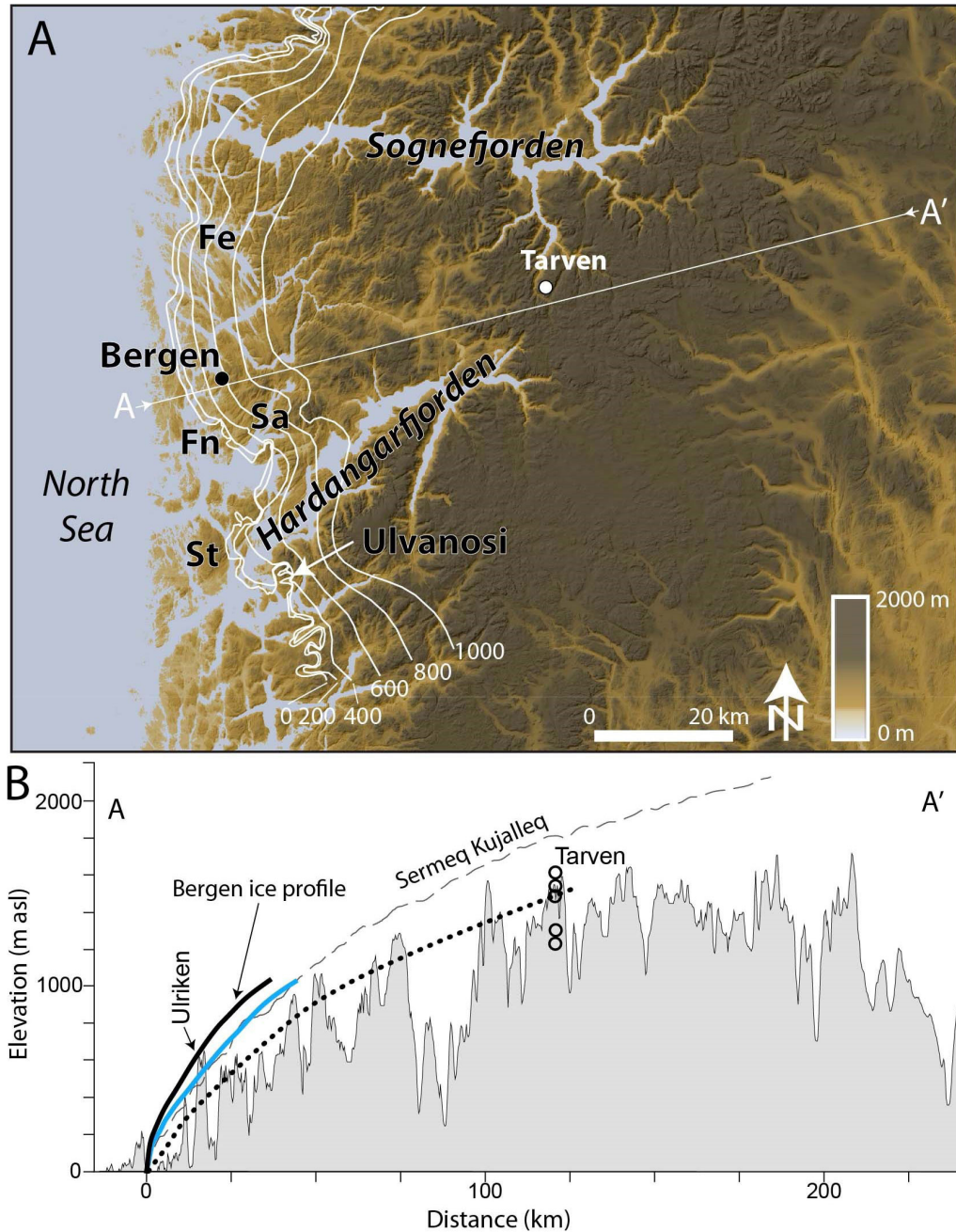
Figure 9. Ice-surface geometry of the Younger Dryas ice configuration in southwestern Norway. Surface contour labels in meters; Fe = Fensfjorden; Sa = Samnangerfjorden; Fn = Fanafjorden; St = Stord. Small circles show dated samples near the head of Sognefjorden on the mountain Tarven. Bottom panel shows relevant ice-sheet profiles; Solid blue line is reconstructed from Hardangerfjorden (Mangerud et al., 2013), dotted is modeled from Fjeldskaar & Amantov (2018); Dashed is measured from the Greenland Ice Sheet at Sermeq Kujalleq. Bergen ice profile shown in black is the reconstruction from this work.

(1) Same ice-sheet width, (2) similar bed of crystalline lithology, and (3) similar underlying topography (Fig. 10). In estimating the Scandinavian Ice Sheet profile, we place the divide to be consistent with regional ice-flow indicators (striae; Rye & Follestad, 1972; Sollid & Torp, 1984). We draw the Scandinavian Ice Sheet height, along a transect from the Bergen area to the Oslo area (Fig. 10), to be about 2500 m a.s.l. to be consistent with southern Greenland's ice-sheet height. We see this reconstruction of the Scandinavian Ice Sheet during the Younger Dryas as a reasonable configuration that is worth further testing.
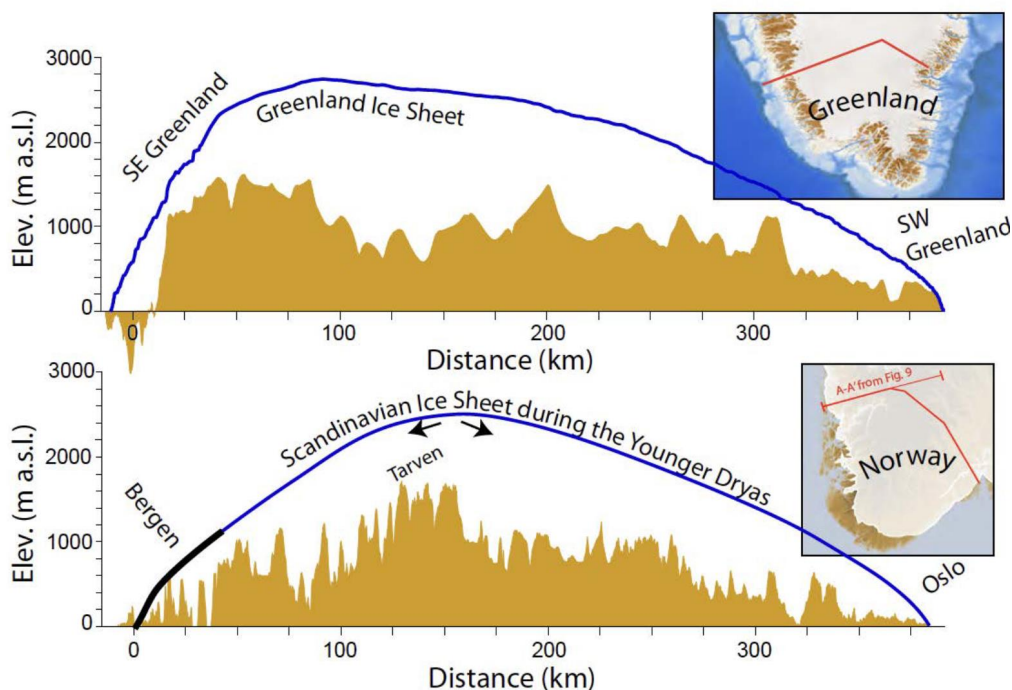
Figure 10. Comparison of southern Greenland (top) with southern Norway (bottom). Each ice-sheet surface is drawn in blue and underlying topography in brown. Note that the age of the Younger Dryas maximum phase may be slightly different in the west and east ends of this transect, but this does not significantly impact the overall shape of this ice-dome reconstruction. Greenland ice surface and bed from layers within the QGreenland QGIS package (Moon et al., 2022; Morlighem et al. 2017). Topography data from Norway are from norgeskart.no. The thick line portion of the Scandinavian Ice Sheet profile is our reconstruction shown in Figure 9.

Conclusions

Beryllium-10 dating of boulders indicates that the summit of the mountain Ulriken (677 m a.s.l.) that towers over the city of Bergen was covered by the Scandinavian Ice Sheet during the Younger Dryas glacier advance. Summits occupied by ice during the Younger Dryas lie only 10–15 km up-flow from the Younger Dryas ice margin and imply an ice-surface slope comparable to what has been found in adjacent fjords. These new constraints on ice-margin geometry add to published field data and, with a comparison to the modern analog of the Greenland Ice Sheet, lead to our best-estimate of an ice-sheet configuration in southern Norway during the Younger Dryas. We find evidence for relatively inefficient erosion at low elevations in the Bergen valleys, which may relate to the protected nature as regional ice flow was across, not along, the investigated valleys. These new field constraints of ice-sheet configuration and basal conditions can assist in improving numerical simulations of ice-sheet processes and history.

Author Contributions.

JB, JM and JIS wrote the manuscript; all authors edited the manuscript. JM, JIS, HL and SOD collected the samples. JB, HL and DF performed the laboratory analysis. JB calculated ages and drafted figures and tables. RG provided map support and georeferenced ice-surface contours. HL and SOD collected the BER samples; JM and JIS collected all others.

References

Aarseth, I. & Mangerud, J. 1974: Younger Dryas end moraines between Hardangerfjorden and Sogne-fjorden, Western Norway. *Boreas 3*, 3–22. https://doi.org/10.1111/j.1502-3885.1974.tb00663.x

Aakesson, H., Gyllencreutz, R., Mangerud, J., Svendsen, J.I., Nick, F.M. & Nisancioglu, K.H. 2020: Rapid retreat of a Scandinavian marine outlet glacier in response to warming at the last glacial termination. *Quaternary Science Reviews 250,* 106645. https://doi.org/10.1016/j.quascirev.2020.106645

Aakesson, H., Morlighem, M., Nisancioglu, K.H., Svendsen, J.I. & Mangerud, J. 2018: Atmosphere-driven ice sheet mass loss paced by topography: Insights from modelling the south-western Scandinavian Ice Sheet. *Quaternary Science Reviews 195,* 32–47. https://doi.org/10.1016/j.quascirev.2018.07.004

Alsos, I.G., Rijal, D.P., Ehrich, D., Karger, D.N., Yoccoz, N.G., Heintzman, P.D., Brown, A.G., Lammers, Y., Pellissier, L., Alm, T., Bråthen, K.A., Coissac, E., Merkel, M.K.F., Alberti, A., Denoeud, F., Bakke, J. & PhyloNorway Consortium. 2022: Postglacial species arrival and diversity buildup of northern ecosystems took millennia. *Sci Adv 8,* eabo7434–eabo7434. https://doi.org/10.1126/sciadv.abo7434

Andersen, J.L., Egholm, D.E., Knudsen, M.F., Linge, H., Jansen, J.D., Pedersen, V.K & Nielsen, S.B. 2018: Widespread Erosion on High Plateaus during Recent Glaciations in Scandinavia. *Nature Communications 9*, 830. https://doi.org/10.1038/s41467-018-03280-2

Balco, G., Stone, J.O., Lifton, N.A. & Dunai, T.J. 2008: A complete and easily accessible means of calculating surface exposure ages or erosion rates from 10Be and 26Al measurements. *Quaternary Geochronology 3*, 174–195. https://doi.org/10.1016/j.quageo.2007.12.001

Bondevik, S. & Mangerud, J. 2002: A Calendar Age Estimate of a Very Late Younger Dryas Ice Sheet Maximum in Western Norway. *Quaternary Science Reviews 21*, 1661–76. https://doi.org/10.1016/S0277-3791(01)00123-8

Borchers, B., Marrero, S., Balco, G., Caffee, M., Goehring, B., Lifton, N., Nishiizumi, K., Phillips, F., Schaefer, J. & Stone, J. 2016: Geological calibration of spallation production rates in the CRONUS-Earth project. *Quaternary Geochronology 31*, 188–198. https://doi.org/10.1016/j.quageo.2015.01.009

Brendryen, J., Haflidason, H., Yokoyama, Y., Haaga, K.A. & Hannisdal, B. 2020: Eurasian Ice Sheet collapse was a major source of Meltwater Pulse 1A 14,600 years ago. *Nature Geoscience 13*, 363–368. https://doi.org/10.1038/s41561-020-0567-4

Briner, J.P., Goehring, B.M., Mangerud, J. & Svendsen, J.I. 2016: The deep accumulation of10Be at Utsira, southwestern Norway: Implications for cosmogenic nuclide exposure dating in peripheral ice sheet landscapes. *Geophysical Research Letters 43,* 9121–9129. https://doi.org/10.1002/2016gl070100

Briner, J.P., Miller, G.H., Davis, P.T. & Finkel, R.C. 2005: Cosmogenic exposure dating in arctic glacial landscapes: implications for the glacial history of northeastern Baffin Island, Arctic Canada. *Canadian Journal of Earth Sciences 42,* 67–84. https://doi.org/10.1139/e04-102

Brook, E.J., Nesje, A., Lehman, S.J., Raisbeck, G.M. & Yiou, F. 1996: Cosmogenic nuclide exposure ages along a vertical transect in western Norway: Implications for the height of the Fennoscandian ice sheet. *Geol 24*, 207. https://doi.org/10.1130/0091-7613(1996)024<0207:CNEAAA>2.3.CO;2

Caron, L., Ivins, E.R., Larour, E., Adhikari, S., Nilsson, J. & Blewitt, G. 2018: GIA Model Statistics for GRACE Hydrology, Cryosphere, and Ocean Science. *Geophysical Research Letters 45,* 2203–2212. https://doi.org/10.1002/2017gl076644

Clark, C.D., Ely, J.C., Hindmarsh, R.C.A., Bradley, S., Ignéczi, A., Fabel, D., Ó Cofaigh, C., Chiverrell, R.C., Scourse, J., Benetti, S., Bradwell, T., Evans, D.J.A., Roberts, D.H., Burke, M., Callard, S.L., Medialdea, A., Saher, M., Small, D., Smedley, R.K., Gasson, E., Gregoire, L., Gandy, N., Hughes, A.L.C., Ballantyne, C., Bateman, M.D., Bigg, G.R., Doole, J., Dove, D., Duller, G.A.T., Jenkins, G.T.H., Livingstone, S.L., McCarron, S., Moreton, S., Pollard, D., Praeg, D., Sejrup, H.P., Van Landeghem, K.J.J. & Wilson, P. 2022: Growth and retreat of the last British–Irish Ice Sheet, 31 000 to 15 000 years ago: the BRITICE-CHRONO reconstruction. *Boreas 51,* 699–758. https://doi.org/10.1111/bor.12594

Corbett, L.B., Bierman, P.R. & Rood, D.H. 2016: An approach for optimizing in situ cosmogenic [10]Be sample preparation. *Quaternary Geochronology 33,* 24–34. https://doi.org/10.1016/j.quageo.2016.02.001

Dalton, April S., Martin Margold, Chris R. Stokes, Lev Tarasov, Arthur S. Dyke, Roberta S. Adams, Serge Allard, et al. 2020: An Updated Radiocarbon-Based Ice Margin Chronology for the Last Deglaciation of the North American Ice Sheet Complex. *Quaternary Science Reviews 234*, 106223. https://doi.org/10.1016/j.quascirev.2020.106223

England, J. 1999: Coalescent Greenland and Innuitian ice during the Last Glacial Maximum: revising the Quaternary of the Canadian High Arctic. *Quaternary Science Reviews 18,* 421–456. https://doi.org/10.1016/s0277-3791(98)00070-5

Fabel, D., Fink, D., Fredin, O., Harbor, J., Land, M., & Stroeven, A.P. 2006: Exposure ages from relict lateral moraines overridden by the Fennoscandian ice sheet. *Quaternary Research 65,* 136–146. https://doi.org/10.1016/j.yqres.2005.06.006

Fareth, O.W. 1972: Geologic map of the Teller Quadrangle, western Seward Peninsula, Alaska. *US Geological Survey.* https://doi.org/10.3133/i685

Fjeldskaar, W. & Amantov, A. 2018: Younger Dryas Transgression in Western Norway: A Modelling Approach. *Norwegian Journal of Geology 98*, 127–39. https://dx.doi.org/10.17850/njg98-1-08

Follestad, B.A. 1972: The Deglaciation of the South-Western Part of the Folgefonn Peninsula, Hordaland.

Goehring, B.M., Brook, E.J., Linge, H., Raisbeck, G.M. & Yiou, F. 2008: Beryllium-10 exposure ages of erratic boulders in southern Norway and implications for the history of the Fennoscandian Ice Sheet. *Quaternary Science Reviews 27*, 320–336. https://doi.org/10.1016/j.quascirev.2007.11.004

Goehring, B.M., Lohne, Ø.S., Mangerud, J., Svendsen, J.I., Gyllencreutz, R., Schaefer, J. & Finkel, R., 2011: Late glacial and holocene 10 Be production rates for western Norway. *Journal of Quaternary Science 27,* 89–96. https://doi.org/10.1002/jqs.1517

Goehring, B.M., Lohne, Ø.S., Mangerud, J., Svendsen, J.I., Gyllencreutz, R., Schaefer, J. & Finkel, R. 2012: Erratum: Late glacial and holocene10Be production rates for western Norway. *Journal of Quaternary Science 27,* 544–544. https://doi.org/10.1002/jqs.2548

Gowan, E.J., Zhang, X., Khosravi, S., Rovere, A., Stocchi, P., Hughes, A.L.C., Gyllencreutz, R., Mangerud, J., Svendsen, J.-I. & Lohmann, G. 2021: A new global ice sheet reconstruction for the past 80 000 years. *Nature Communications 12,* 1199–1199. https://doi.org/10.1038/s41467-021-21469-w

Heaton, T.J., Köhler, P., Butzin, M., Bard, E., Reimer, R.W., Austin, W.E.N., Bronk Ramsey, C., Grootes, P.M., Hughen, K.A., Kromer, B., Reimer, P.J., Adkins, J., Burke, A., Cook, M.S., Olsen, J. & Skinner, L.C. 20: Marine20—The Marine Radiocarbon Age Calibration Curve (0–55,000 cal BP). *Radiocarbon 62*, 779–820. https://doi.org/10.1017/rdc.2020.68

Hamborg, M., Mangerud, J., 1981: En rekonstruksjon av isbevegelser under siste istid i Samnanger og Kvam, Hordaland, Vest-Norge (With English Summary: A reconstruction of ice movement directions during the Late Weichselian in Samnanger and Kvam, Hordaland, Western Norway). *Norges geologiske undersøkelse 369,* 77-98.

Hughes, A.L.C., Gyllencreutz, R., Lohne, Ø.S., Mangerud, J. & Svendsen, J.I. 2015: The last Eurasian ice sheets – a chronological database and time-slice reconstruction, DATED-1. *Boreas 45,* 1–45. https://doi.org/10.1111/bor.12142

Kohl, C.P. & Nishiizumi, K. 1992: Chemical isolation of quartz for measurement of in-situ -produced cosmogenic nuclides. *Geochimica et Cosmochimica Acta 56,* 3583–3587. https://doi.org/10.1016/0016-7037(92)90401-4

Lal, D. 1991: Cosmic ray labeling of erosion surfaces: in situ nuclide production rates and erosion models. *Earth and Planetary Science Letters 104*, 424–439. https://doi.org/10.1016/0012-821x(91)90220-c

Lohne, Ø.S., Bondevik, S., Mangerud, J. & Schrader, H. 2004: Calendar Year Age Estimates of Allerød–Younger Dryas Sea-Level Oscillations at Os, Western Norway. *Journal of Quaternary Science 19*, 443–64. https://doi.org/10.1002/jqs.846

Lohne, Ø.S., Bondevik, S., Mangerud, J. & Svendsen, J.I. 2007: Sea-level fluctuations imply that the Younger Dryas ice-sheet expansion in western Norway commenced during the Allerød. *Quaternary Science Reviews 26*, 2128–2151. https://doi.org/10.1016/j.quascirev.2007.04.008

Mangerud, J. 2023: Younger Dryas Stadial (YD) Local Moraines in Western and Northern Norway." In *European Glacial Landscapes*, 453–58. Elsevier. https://doi.org/10.1016/B978-0-323-91899-2.00061-9

Mangerud, J. & Svendsen, J.I., 2017: The Holocene Thermal Maximum around Svalbard, Arctic North Atlantic; molluscs show early and exceptional warmth. *The Holocene 28,* 65–83. https://doi.org/10.1177/0959683617715701

Mangerud, J., Sejrup, H.P., Sønstegaard, E. & Haldorsen, S. 1981: A continuous Eemian-Early Weichselian sequence containing pollen and marine fossils at Fjøsanger, western Norway. Boreas 10, 137–208. https://doi.org/10.1111/j.1502-3885.1981.tb00479.x

Mangerud, J., Goehring, B.M., Lohne, Ø.S., Svendsen, J.I. & Gyllencreutz, R. 2013: Collapse of marine-based outlet glaciers from the Scandinavian Ice Sheet. *Quaternary Science Reviews 67,* 8–16. https://doi.org/10.1016/j.quascirev.2013.01.024

Mangerud, J., Aarseth, I., Hughes, A.L.C., Lohne, Ø.S., Skår, K., Sønstegaard, E. & Svendsen, J.I. 2016: A major re-growth of the Scandinavian Ice Sheet in western Norway during Allerød-Younger Dryas. *Quaternary Science Reviews 132*, 175–205. https://doi.org/10.1016/j.quascirev.2015.11.013

Mangerud, J., Briner, J.P., Goslar, T. & Svendsen, J.I. 2017: The Bølling-age Blomvåg Beds, western Norway: implications for the Older Dryas glacial re-advance and the age of the deglaciation. *Boreas 46,* 162–184. https://doi.org/10.1111/bor.12208

Mangerud, J., Hughes, A.L.C., Sæle, T.H. & Svendsen, J.I. 2019: Ice-flow patterns and precise timing of ice sheet retreat across a dissected fjord landscape in western Norway. *Quaternary Science Reviews 214*, 139–163. https://doi.org/10.1016/j.quascirev.2019.04.032

Moon, T., Fisher, M., Stafford, T. & Harden, L. 2020: QGreenland: Enabling Science through GIS. https://doi.org/10.1002/essoar.10504079.1

Morlighem, M., Williams, C.N., Rignot, E., An, L., Arndt, J.E., Bamber, J.L., Catania, G., Chauché, N., Dowdeswell, J.A., Dorschel, B., Fenty, I., Hogan, K., Howat, I., Hubbard, A., Jakobsson, M., Jordan, T.M., Kjeldsen, K.K., Millan, R., Mayer, L., Mouginot, J., Noël, B.P.Y., O'Cofaigh, C., Palmer, S., Rysgaard, S., Seroussi, H., Siegert, M.J., Slabon, P., Straneo, F., van den Broeke, M.R., Weinrebe, W., Wood, M. & Zinglersen, K.B. 2017: BedMachine v3: Complete Bed Topography and Ocean Bathymetry Mapping of Greenland From Multibeam Echo Sounding Combined With Mass Conservation. *Geophysical Research Letters 44,* 11051–11061. https://doi.org/10.1002/2017GL074954

Nesje, A. 2002: A large rockfall avalanche in Oldedalen, inner Nordfjord, western Norway, dated by means of a sub-avalanche Salix sp. tree trunk. *Norwegian Journal of Geology 82*, 59–62.

Regnéll, C., Briner, J.P., Haflidason, H., Mangerud, J. & Svendsen, J.I. 2021: Deglaciation of the Scandinavian Ice Sheet and a Younger Dryas ice cap in the outer Hardangerfjorden area, southwestern Norway. *Boreas 51*, 255–273. https://doi.org/10.1111/bor.12568

Rye, N. & Follestad, B. A. 1972: The ice movement and the ice divide in the Hardangervidda area. *Norges Geologiske Undersøkelse 280*, 25–30.

Sejrup, H.P. & Hjelstuen, B.O. 2022: The North Sea and Mid–Norwegian continental margin: glacial landforms from the Last Glacial Maximum. *European Glacial Landscapes 2022,* 401–406. https://doi.org/10.1016/b978-0-12-823498-3.00063-7

Sejrup, H.P., Larsen, E., Haflidason, H., Berstad, I.M., Hjelstuen, B.O., Jonsdottir, H.E., King, E.L., Landvik, J., Longva, O., Nygård, A., Ottesen, D., Raunholm, S., Rise, L. & Stalsberg, K. 2003: Configuration, history and impact of the Norwegian Channel Ice Stream. *Boreas 32*, 18–36. https://doi.org/10.1080/03009480310001029

Sollid, J.L., Carlson, A.B. & Torp, B. 1980: Trollheimen – Sunndalsfjella – Oppdal Kvartærgeologisk kart 1:100 000 Kort beskrivelse til kartet Trollheimen – Sunndalsfjella – Oppdal Quarternary map 1:100000 Short description of the map. *Norwegian Journal of Geography 34,* 177–189. https://doi.org/10.1080/00291958008621912

Sommers, A.N., Otto-Bliesner, B.L., Lipscomb, W.H., Lofverstrom, M., Shafer, S.L., Bartlein, P.J., Brady, E.C., Kluzek, E., Leguy, G., Thayer-Calder, K. & Tomas, R.A. 2021: Retreat and Regrowth of the Greenland Ice Sheet During the Last Interglacial as Simulated by the CESM2-CISM2 Coupled Climate–Ice Sheet Model. *Paleoceanography and Paleoclimatology 36.* https://doi.org/10.1029/2021pa004272

Stone, J.O. 2000: Air pressure and cosmogenic isotope production. Journal of Geophysical Research. *Solid Earth 105*, 23753–23759. https://doi.org/10.1029/2000jb900181

Stroeven, A.P., Heyman, J., Fabel, D., Björck, S., Caffee, M.W., Fredin, O. & Harbor, J.M. 2015: A new Scandinavian reference 10Be production rate. *Quaternary Geochronology 29,* 104–115. https://doi.org/10.1016/j.quageo.2015.06.011

Wirsig, C., Ivy-Ochs, S., Reitner, J.M., Christl, M., Vockenhuber, C., Bichler, M. & Reindl, M. 2017: Subglacial Abrasion Rates at Goldbergkees, Hohe Tauern, Austria, Determined from Cosmogenic 10Be and 36Cl Concentrations. *Earth Surface Processes and Landforms 42*, 1119–31. https://doi.org/10.1002/esp.4093

Young, N.E., Schaefer, J.M., Briner, J.P. & Goehring, B.M., 2013: A 10Be production-rate calibration for the Arctic. *Journal of Quaternary Science 28,* 515–526. https://doi.org/10.1002/jqs.2642